SLAC-PUB-5660
December 1991
(E)

BACKGROUNDS AND MASKING AT THE TAU-CHARM FACTORY

DAVID P. STOKER
Stanford Linear Accelerator Center, Stanford, CA 94309.

Abstract

Preliminary results are presented for beam-related backgrounds in the Tau-Charm Factory detector. The Orsay flat-beam optics design was used in the simulations. Results with different masking schemes are compared for lost beam particle backgrounds.

1. INTRODUCTION

Backgrounds at a Tau-Charm Factory may originate from several sources including synchrotron radiation, lost beam particles, beam-gas events, and zero-angle radiative Bhabha events. "Lost" beam particles refer to electrons or positrons which undergo Coulomb scattering or bremsstrahlung from residual gas molecules and strike the beam-pipe or masks. The backgrounds in the detector depend strongly on the machine optics and the masking near the interaction point. I have made much use of the procedures and programs used in the background studies for the B-Factory proposed by SLAC/LBL.

The Orsay flat-beam optics design[1] was used for the present studies. The floor-layout is shown in Fig. 1. The optics elements closest to the IP are given in Table 1. Q1 and Q2 are quadrupoles, ESEP is the electrostatic separator, and BV1 is a vertical bend dipole magnet. The field strengths given for ESEP and BV1 assume the beam energy is 2.0 GeV. The beam-pipe was assumed to have a radius of 6 cm in the interaction region and 4 cm elsewhere.

Table 1. Orsay flat-beam optics elements near the IP.

Element	Distance from IP (m)	Strength ($E_b = 2.0\,\mathrm{GeV}$)
Q1	$0.8 - 1.4$	$K = -2.846\,\mathrm{m}^{-2}$
Q2	$1.7 - 2.3$	$K = 1.521\,\mathrm{m}^{-2}$
ESEP	$2.6 - 7.3$	$E = 2.56\,\mathrm{MV/m}$
BV1	$10.8 - 11.8$	$B = 0.1334\,\mathrm{T}$

The beam at the IP has $\sigma_x = 480\,\mu\mathrm{m}$, $\sigma_y = 6\,\mu\mathrm{m}$, $\sigma_{x'} = \sigma_{y'} = 0.60\,\mathrm{mradians}$. The simulations assume each bunch contains 1.4×10^{11} electrons or positrons, and a bunch crossing rate of 20 MHz.

All background results given in the following sections are for 2.0 GeV beam energy. The lost beam particle simulations assumed scattering from residual gas equivalent to 5 nTorr of nitrogen (N_2).

*Work supported by the Department of Energy, contract DE-AC03-76SF00515
Invited talk presented at the Meeting on Tau-Charm Factory Detector and Machine, Seville, Spain, April 29-May 2, 1991

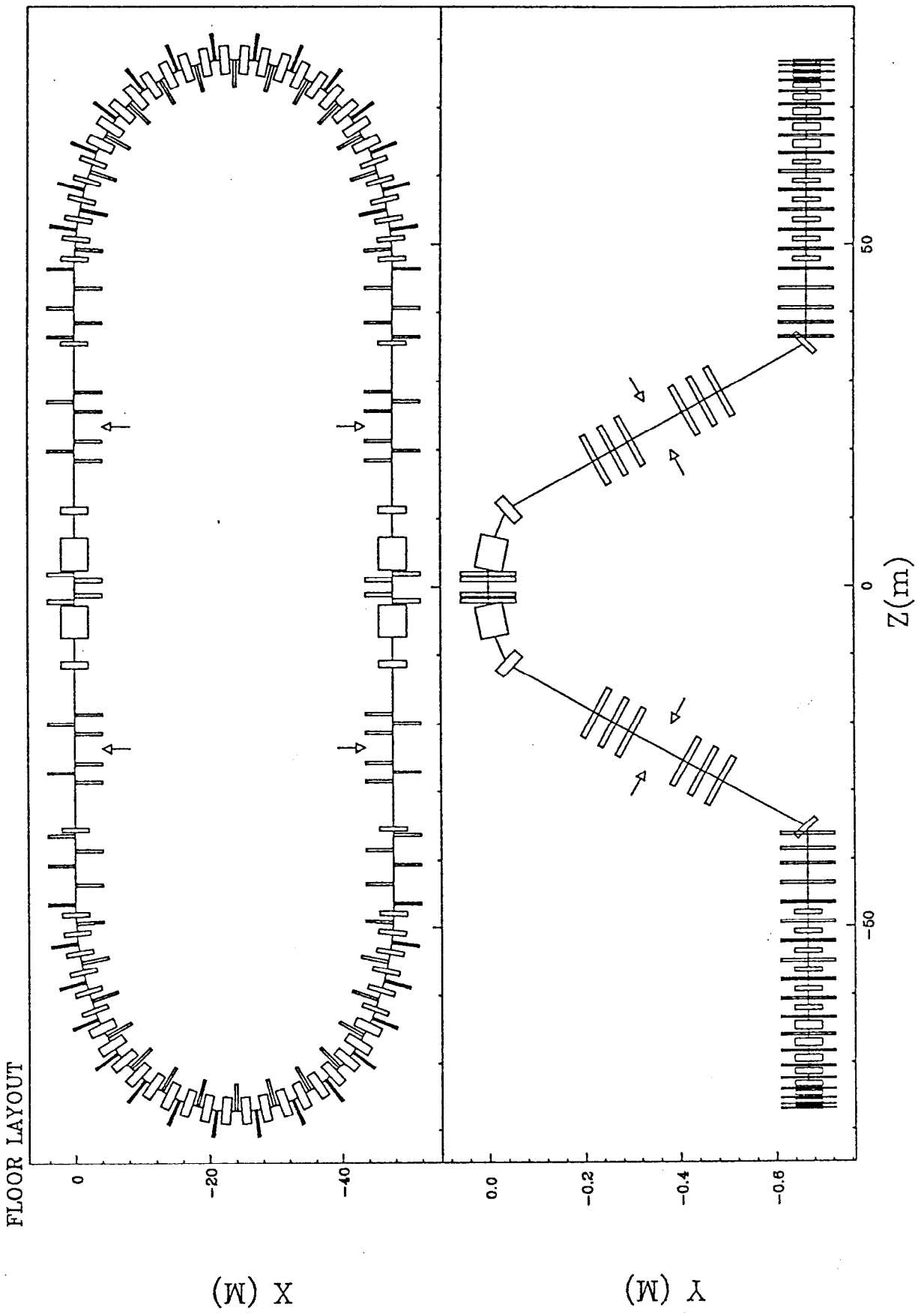

Fig. 1. Floor layout of the Orsay flat-beam optics design.

2. SYNCHROTRON RADIATION

Each of the optics elements in Table 1 generates synchrotron radiation which strikes the beam-pipe. The following results are for the beam moving in the $+z$ direction towards the IP ($z = 0$) through the optics elements at $z < 0$.

The average number of photons radiated by a relativistic electron in a uniform magnetic field is

$$N_a = \frac{5}{2\sqrt{3}}\alpha\gamma\theta \tag{1}$$

When the bend angle θ is small and the electron's motion is perpendicular to a field of strength B (Tesla) in a region of length L (meters)

$$N_a = 6.18BL \tag{2}$$

and the critical energy k_c (keV) of the photons radiated from an electron of energy E_b (GeV) is

$$k_c = 0.666E_b^2B \tag{3}$$

The average energy of the photons is $k_a = 0.31k_c$.

The synchrotron radiation from the vertical bend elements BV1 and ESEP was calculated from equations (1)-(3). Here ESEP's 2.56 MV/m electric field was approximated by an 85 Gauss magnetic field.

BV1 upstream of the IP illuminates a 6 cm radius beam-pipe from $z = -7.6$ m to $z = 5.0$ m with 2.4×10^{12} photons/μs with critical energy $k_c = 355$ eV. The electrostatic separators (ESEP) should be shielded from this radiation to reduce photo-electron currents and possible sparking problems. The low critical energy of these photons should allow simple masking and absorption in the beam-pipe to prevent significant detector backgrounds.

ESEP upstream of the IP illuminates the beam-pipe downstream of the IP at $z >$ 5.0 m with 6.8×10^{11} photons/μs with critical energy $k_c = 23$ eV. This radiation therefore does not reach the beam-pipe near the IP, but would reach the other separator in the absence of appropriate shielding.

Synchrotron radiation from Q1 and Q2 was calculated using the program SSYNC4 which is a variant of QSRAD. The beam was cut off at 10σ, and had no additional tails. The resulting synchrotron radiation with energy greater than 10 eV which reaches a radius of 6 cm in the regions of the IP, Q1, Q2, and ESEP is shown in Table 2. The synchrotron radiation has a low average energy and reaches the beam-pipe radius well downstream of the IP in the region of ESEP.

To summarize, (i) the vertical bend magnet BV1 is the only direct source of synchrotron radiation ($k_c = 355$ eV) for the beam-pipe at the IP, (ii) BV1, ESEP, and the quadrupoles are all sources of synchrotron radiation reaching the region of the electrostatic separators, which will require appropriate shielding.

Table 2. Synchrotron radiation from Orsay flat-beam optics quadrupoles.

z (m)	N_γ/μs ($E > 10$ eV)	E_{av} (keV)	N_γ/μs ($E > 1.0$ keV)
< 0.8	0	0	0
$0.8 - 1.7$	0	0	0
$1.7 - 2.6$	2.8×10^{-10}	0.15	6.4×10^{-12}
$2.6 - 7.3$	8.2×10^{6}	0.07	1.6×10^{3}

3. BEAM-GAS BACKGROUND

Beam-gas backgrounds may be estimated from the rates observed at existing machines. Data from the Mark III at SPEAR was used by R. Schindler[2] to estimate the probability for a beam-gas event particle with transverse momentum greater than p_T (MeV/c) to enter the detector to be $P_{bg} = 0.034 \exp(-p_T/16.3)$ per beam crossing.

For example, since only particles with $p_T > 150$ MeV/c will reach the CsI calorimeter if the solenoid field is 1.0 T the rate is predicted to be 3.4×10^{-6} per beam crossing, or 68 Hz for a beam crossing rate of 20 MHz. The CsI would receive a dose of about 1.3×10^{-4} rad/yr if it completely absorbs the particles' energy. In this paper a "year" of running is taken to be 10^7 s.

Similarly, the BGO forward detector would receive a dose of about 22 rad/yr. For comparison, it is estimated that the BGO would receive an average of 5 rad/yr from Bhabha events and 60 rad/yr at its inner edge.

4. LOST BEAM PARTICLES

Electrons and positrons may be lost from the beam by scattering from residual gas molecules in the vacuum chamber. The program DECAY TURTLE was used to simulate both Coulomb scattering where the scattered $e^{\pm}$ retain the full beam energy, and bremsstrahlung where the photon and scattered $e^{\pm}$ energies sum to the beam energy. As noted in the Introduction, the residual gas was assumed to be equivalent to 5 nTorr of N_2 throughout the ring.

The Orsay flat-beam optics file was first converted from MAD to TRANSPORT format and then further modified for use with DECAY TURTLE by adding the appropriate control cards and specifying apertures corresponding to the beam-pipe and masks. The range of $e^{\pm}$ scattering angles used in Coulomb scattering was from 1.0 mradians to 500 mradians. The range of $e^{\pm}$ fractional energy loss used in bremsstrahlung was from 0.02 to 0.99. Particles ($e^{\pm}$ or γ) striking apertures within 9 m of the IP had their positions and directions of incidence and their energy recorded. The trajectories were then linearly extrapolated to find the corresponding hits on the beam-pipe or masks. These rays were then used as input to an EGS simulation of the beam-pipe, masking, and detector.

The EGS simulation made use of the program OBJEGS written by Chris Hearty[3] which creates planar/cylindrical geometry regions from a file specifying the minimum and maximum radius and z coordinates of the detector and mask components. The detector geometry used in the simulation was based on the "P5" layout. The EGS simulation included the detector's 1.0 T solenoidal field, and also the fields of Q1, Q2, and ESEP. Since there was no means of superposing these fields, the latter took precedence over the solenoid field in regions where both should be present. It should be noted that a better approximation can be obtained by slicing-up the overlapping field regions and interleaving the two field types with double their real strengths. This method was used for the zero-angle radiative Bhabha study (section 5), and will be used in future lost beam particle studies.

We consider the scattered $e^{\pm}$ or photons which strike the 6 cm radius beam-pipe within 8.5 m of the interaction point. The energy of these scattered particles from one beam moving in the positive z direction is shown in Fig. 2 according to the location of the scattering event relative to the IP. Almost all the incident particles originate from scattering within 50 m of the IP. Comparison with Fig. 1 shows this corresponds approximately to the region between the last horizontal bend and the IP.

In Fig. 3 the energy of the scattered particles is shown according to where it strikes the beam-pipe relative to the IP. Figure 3(a) shows photons only, and Figure 3(b) shows e^{-} only. The photon energy peak near $z = -7.5$ m is due to bremsstrahlung in the inclined straight section upstream of BV1, while the peak near $z = 5.0$ m is due to bremsstrahlung between BV1 and ESEP. The electron energy peaks near $z = -2$ m and $z = 1$ m correspond to off-axis and/or off-energy e^{-} being over-focussed or over-defocussed by the quadrupoles Q1 and Q2. It should be noted that the vertical bend elements BV1 and ESEP in our two-ring design over-bend off-energy beam particles entering the interaction region. These particles may then strike the beam-pipe before reaching the quadrupoles, or may do so as a result of entering the quadrupoles well off-axis.

Three masking schemes were considered. They are specified in Table 3 and shown in Fig. 4. In each case the masks are tungsten and the quadrupoles are assumed to iron 6.0 cm thick. Masks 1 and 2 provide 2.0 cm of tungsten outside the beam-pipe between Q1 and Q2, and outboard of Q2. Mask 3 is intended to provide extra shielding against photons which would hit the beam-pipe near $|z| = 7.5$ m (see Fig. 3(a)) and against far off-axis $e^{\pm}$. Mask 4 is intended to provide extra shielding against $e^{\pm}$ which would hit the beam-pipe near the quadrupoles and the IP (see Fig. 3(b)). These simple masking schemes ignore the electrostatic separators, vacuum pumps, feed-throughs, and other instrumentation which would be present in the real interaction region.

The results of the EGS simulations of lost beam particle backgrounds for the three masking schemes are given in Table 4. The numbers of photons and $e^{\pm}$ per μs striking the Be beam-pipe, the BGO forward detector, and the CsI calorimeter are listed. The energy deposited (MeV/μs) in the BGO, drift-chamber gas, TOF, and CsI are also given together with the corresponding radiation doses (rad/yr) for the BGO, TOF, and CsI, and the charge deposited on the drift-chamber wires (C/cm/yr).

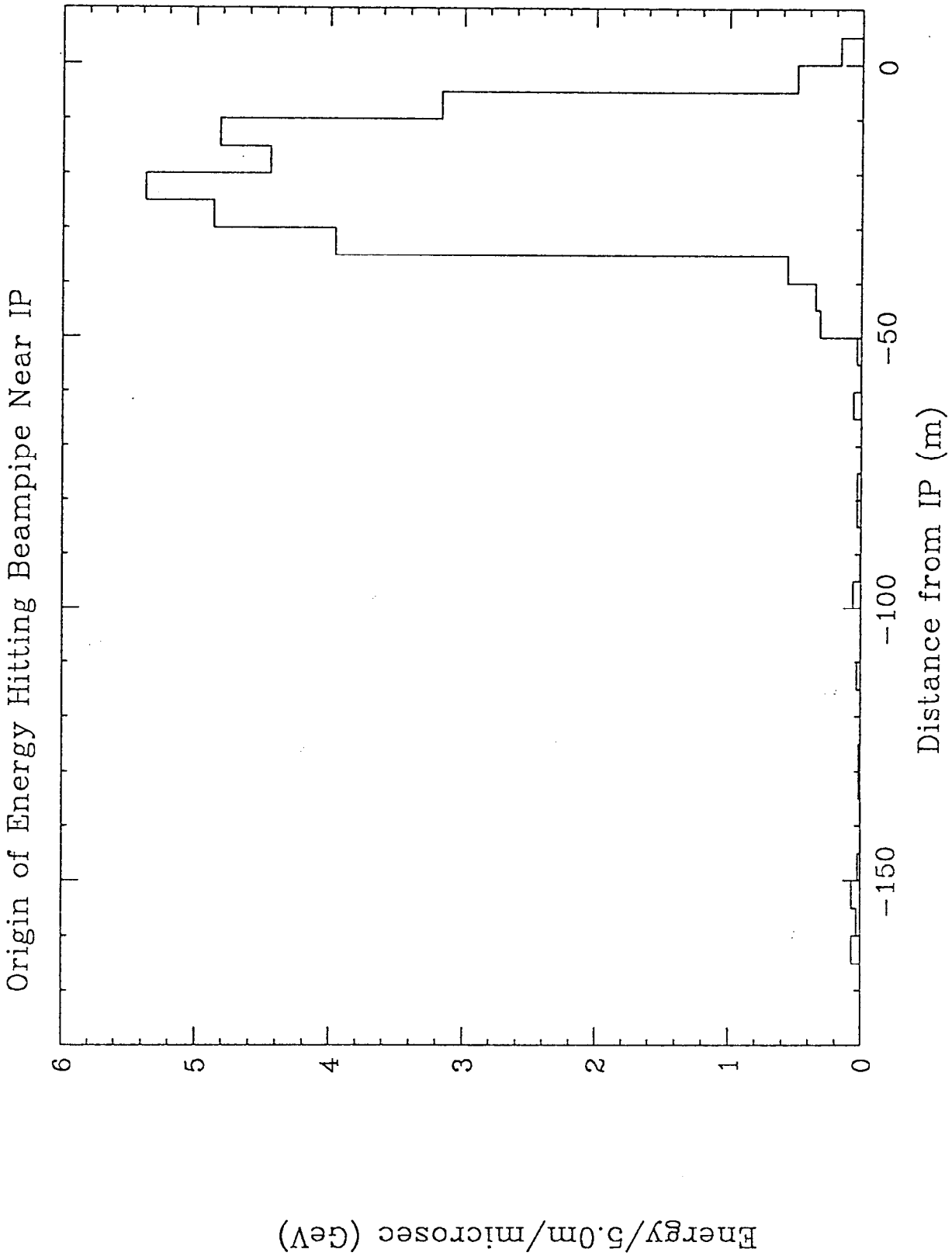

Fig. 2. Energy of scattered e^- or photons which strike the beam-pipe within 8.5 m of the IP, displayed according to location of scattering event.

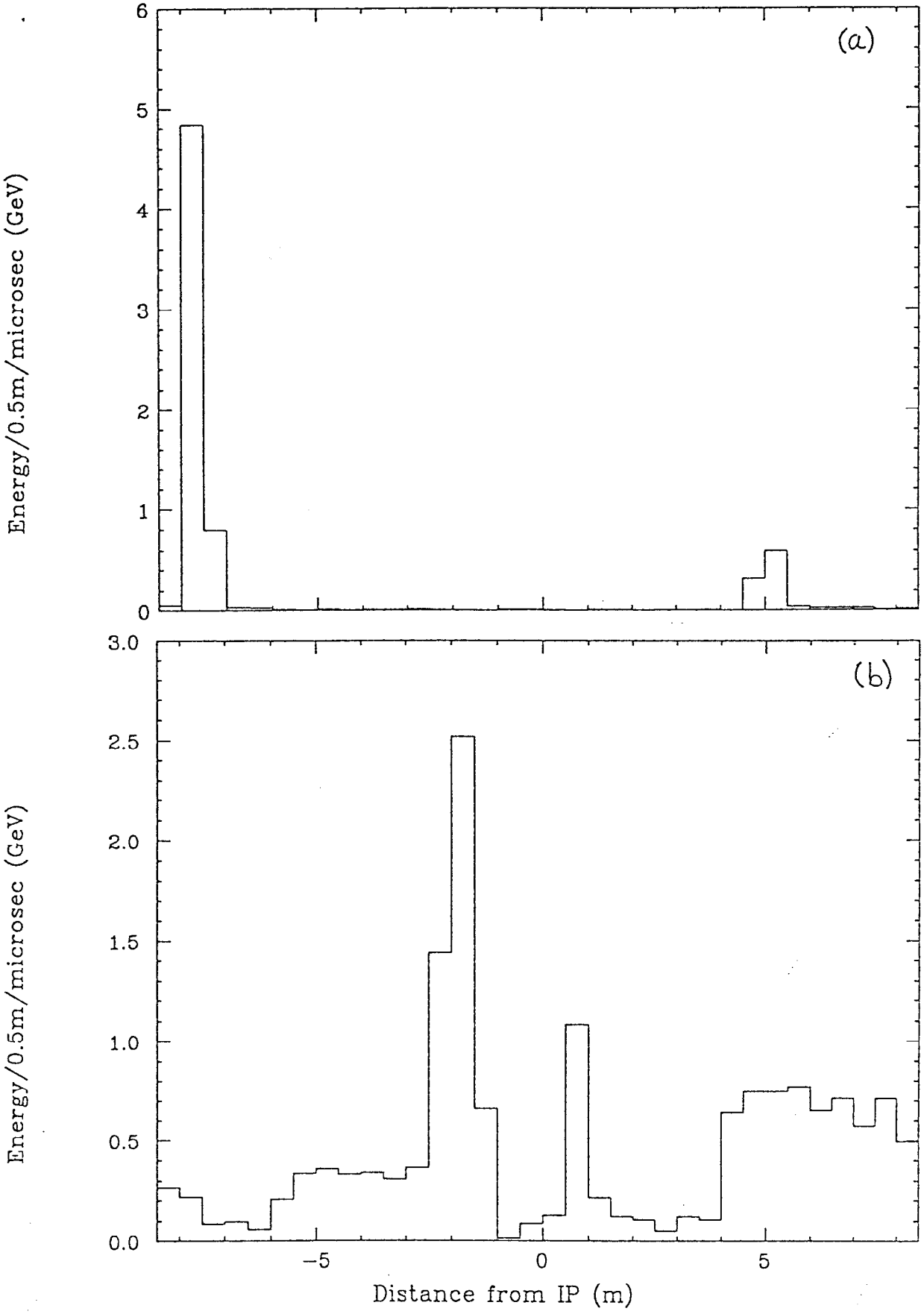

Fig. 3. Energy of scattered photons (a) and scattered e^- (b) displayed according to distance of hits on beam-pipe from IP.

Table 3. Beam-pipe, quadrupoles, and masks in EGS simulations.

Material	Scheme A	Scheme B	Scheme C
Beam-pipe (Be)	$-0.8 < z < 0.8$m $6.0 < r < 6.18$cm	$-0.8 < z < 0.8$m $6.0 < r < 6.18$cm	$-0.8 < z < 0.8$m $6.0 < r < 6.18$cm
Beam-pipe (Al)	$0.8 < \|z\| < 9.0$m $6.0 < r < 6.25$cm	$0.8 < \|z\| < 9.0$m $6.0 < r < 6.25$cm	$0.8 < \|z\| < 9.0$m $6.0 < r < 6.25$cm
Q1 (Fe)	$0.8 < \|z\| < 1.4$m $6.25 < r < 12.25$cm	$0.8 < \|z\| < 1.4$m $6.25 < r < 12.25$cm	$0.8 < \|z\| < 1.4$m $6.25 < r < 12.25$cm
Q2 (Fe)	$1.7 < \|z\| < 2.3$m $6.25 < r < 12.25$cm	$1.7 < \|z\| < 2.3$m $6.25 < r < 12.25$cm	$1.7 < \|z\| < 2.3$m $6.25 < r < 12.25$cm
Mask 1 (W)	$1.4 < \|z\| < 1.7$m $6.25 < r < 8.25$cm	$1.4 < \|z\| < 1.7$m $6.25 < r < 8.25$cm	$1.4 < \|z\| < 1.7$m $6.25 < r < 8.25$cm
Mask 2 (W)	$2.3 < \|z\| < 9.0$m $6.25 < r < 8.25$cm	$2.3 < \|z\| < 9.0$m $6.25 < r < 8.25$cm	$2.3 < \|z\| < 9.0$m $6.25 < r < 8.25$cm
Mask 3 (W)		$8.0 < \|z\| < 7.9$m $4.0 < r < 6.0$cm	$7.9 < \|z\| < 7.8$m $4.0 < r < 6.0$cm
Mask 4 (W)			$0.5 < \|z\| < 2.4$m $3.5 < r < 6.0$cm

The energy deposited in the inner and main drift-chambers is for the gas alone (assumed to be 1.0 Torr He(78%)/CO_2(15%)/Isobutane(7%)) and ignores the wires. The charge deposited on the wires is an average over each drift-chamber and assumes these energy depositions, 30 eV per primary ion pair, a gain of 5×10^4, and a cell area of 4 cm^2.

The results for masking schemes A and B are quite similar with B being somewhat better than A. However, masking scheme C gives markedly lower backgrounds. While this shows masking inside the beam-pipe near the quadrupoles and IP can improve the detector backgrounds it should be noted that no optimization of mask 4 has been attempted yet, and it may be too restrictive.

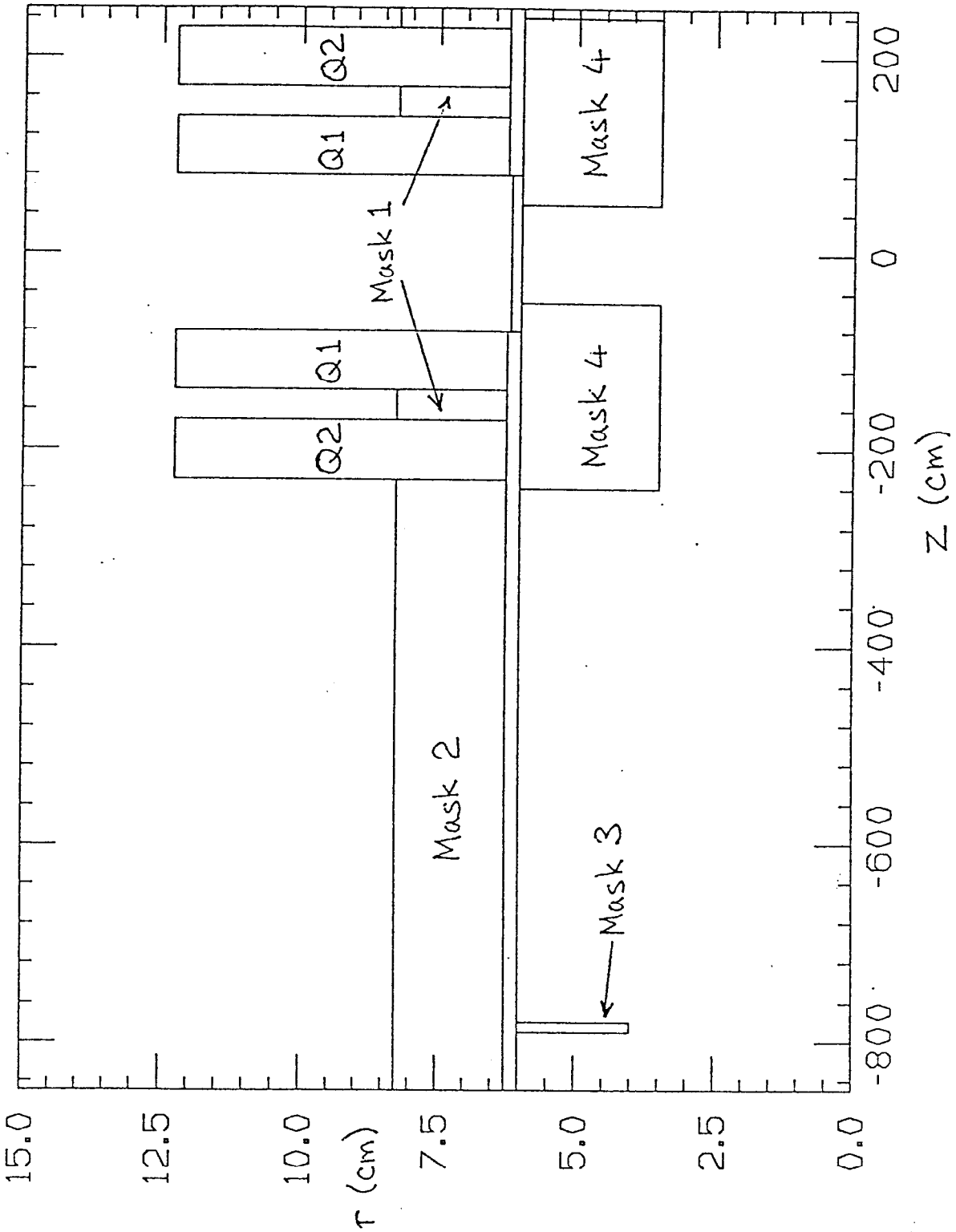

Fig. 4. Beam-pipe, quadrupoles and masks specified in Table 3.

Table 4. Detector backgrounds (particles/μs) from lost beam particles.

Detector Element		Scheme A	Scheme B	Scheme C
Beam-pipe (Be)	N_γ	69.2	57.0	47.0
	$\langle E_\gamma \rangle$ (MeV)	5.31	5.43	3.03
	N_γ ($E > 10$ MeV)	6.4	5.4	0.64
	N_γ ($E > 100$ MeV)	0.58	0.40	< 0.08
	N_e	12.2	10.8	3.8
	$\langle E_e \rangle$ (MeV)	190.5	205.7	46.2
	N_e ($E > 10$ MeV)	3.6	3.4	0.86
	N_e ($E > 100$ MeV)	1.7	1.6	0.20
BGO	N_γ	29.2	24.0	11.4
	$\langle E_\gamma \rangle$ (MeV)	6.19	6.98	6.43
	N_γ ($E > 10$ MeV)	2.9	2.6	0.98
	N_γ ($E > 100$ MeV)	0.30	0.26	0.11
	N_e	2.0	1.7	0.78
	$\langle E_e \rangle$ (MeV)	92.1	121.8	35.0
	N_e ($E > 10$ MeV)	0.80	0.76	0.26
	N_e ($E > 100$ MeV)	0.32	0.30	0.064
	E_{dep} (MeV/μs)	311.	286.	67.8
	Dose (rad/yr)	764.	700.	168.
Inner DC Gas	E_{dep} (MeV/μs)	0.40	0.40	0.16
	Q_{dep} (C/cm/yr)	0.020	0.020	0.0079
Main DC Gas	E_{dep} (MeV/μs)	0.87	0.63	0.18
	Q_{dep} (C/cm/yr)	0.0011	0.0008	0.0002
TOF	E_{dep} (MeV/μs)	68.2	56.8	26.3
	Dose (rad/yr)	2.7	2.3	1.1
CsI Calorimeter	N_γ	110.	92.	49.2
	$\langle E_\gamma \rangle$ (MeV)	1.39	1.41	1.14
	N_γ ($E > 10$ MeV)	1.6	1.5	0.26
	N_e	0.032	< 0.038	0.032
	$\langle E_e \rangle$ (MeV)	8.05	$---$	2.34
	N_e ($E > 10$ MeV)	0.008	< 0.038	< 0.074
	E_{dep} (MeV/μs)	153.	130.	56.2
	Dose (rad/yr)	0.61	0.52	0.23

5. ZERO-ANGLE RADIATIVE BHABHAS

Radiative Bhabha events at essentially zero scattering angle are another source of background. Here one is concerned about events in which the final e^+ or e^-, although travelling in the beam direction, are of sufficiently low energy to be deflected into the beam-pipe or masks by the quadrupoles or electrostatic separators.

Following the work of Blinov *et al.*[4] it is estimated that the zero-angle radiative Bhabha differential rate at the Tau-Charm Factory is

$$\frac{dN}{dE_\gamma} = \frac{1.2 \times 10^8}{E_\gamma} \, \mathrm{s}^{-1} \tag{4}$$

The total rate of e^+ and e^- with energies $E_{min} < E_e < E_{max}$ for a beam energy E_b from zero-angle radiative Bhabhas is then

$$N = 1.2 \times 10^8 \log\left(\frac{E_b - E_{min}}{E_b - E_{max}}\right) \mathrm{s}^{-1} \tag{5}$$

An EGS simulation was performed for these off-energy $e^\pm$ using masking scheme B (Table 3). The $e^\pm$ originated from the IP with the σ_x, σ_y, $\sigma_{x'}$, and $\sigma_{y'}$ characteristic of the initial beam (see Introduction). The results of the simulation are shown in Table 5.

Comparison of Tables 4 and 5 for masking scheme B show that the zero angle radiative Bhabha backgrounds are less than the lost beam particle backgrounds.

Table 5. Detector backgrounds (particles/μsec) from zero-angle radiative Bhabhas.

Detector Element		Scheme B
Beam-pipe	N_γ	0.052
	$\langle E_\gamma \rangle$ (MeV)	0.31
	N_γ ($E > 10$ MeV)	< 0.006
	N_e	< 0.006
	$\langle E_e \rangle$ (MeV)	$---$
BGO	N_γ	0.040
	$\langle E_\gamma \rangle$ (MeV)	0.29
	N_γ ($E > 10$ MeV)	< 0.003
	N_e	0.0026
	$\langle E_e \rangle$ (MeV)	1.47
	N_e ($E > 10$ MeV)	< 0.003
	E_{dep} (MeV/μs)	0.012
	Dose (rad/yr)	0.029
Inner DC Gas	E_{dep} (MeV/μs)	$---$
Main DC Gas	E_{dep} (MeV/μs)	0.021
	Q_{dep} (C/cm/yr)	2.6×10^{-5}
TOF	E_{dep} (MeV/μs)	9.7
	Dose (rad/yr)	0.39
CsI Calorimeter	N_γ	17.5
	$\langle E_\gamma \rangle$ (MeV)	1.40
	N_γ ($E > 10$ MeV)	0.26
	N_e	0.013
	$\langle E_e \rangle$ (MeV)	2.49
	N_e ($E > 10$ MeV)	$< .006$
	E_{dep} (MeV/μs)	24.5
	Dose (rad/yr)	0.098

6. INJECTION

It is anticipated that injection will occur once per hour with a filling-time of 10 minutes for e^+ and less for e^-. Consequently the ratio data-taking time to injection time should be about 5:1. If one arbitrarily assumes that the backgrounds during injection will be 100 times worse than the lost beam particle backgrounds during normal running, then the injection backgrounds can be estimated by multiplying the lost beam particle backgrounds in Table 4 by 100 except for the integrated "Q_{dep}" and "Dose" which should be multiplied by 20.

7. SUMMARY AND CONCLUSIONS

Beam-related backgrounds from several sources have been estimated in the previous sections.

The energy of the synchrotron radiation from the vertical bends and quadrupoles is low enough to allow simple masking and absorption in the beam-pipe to prevent significant detector backgrounds.

The radiation doses in the BGO forward detector, TOF, and CsI calorimeter estimated in the previous sections are summarized in Table 6. The doses in the TOF and CsI are quite low, but the dose expected in the BGO may be of concern.

Table 6. Summary of expected radiation doses.

Detector Element	Background Source	Dose (rad/yr)
BGO	Beam-Gas	22
	Lost beam particles	168
	Zero-angle radiative Bhabhas	0.029
	Bhabhas	5
	Injection	3400
TOF	Lost beam particles	1.1
	Zero-angle radiative Bhabhas	0.39
	Injection	22
CsI	Beam-Gas	1.3×10^{-4}
	Lost beam particles	0.23
	Zero-angle radiative Bhabhas	0.098
	Injection	4.6

The charge deposited on the inner drift-chamber wires during normal running from lost beam particle backgrounds is expected to be about 10^{-2} C/cm/yr on average, which is well below the level of about 1 C/cm at which ageing effects become a problem. If the integrated injection backgrounds are about 20 times the lost beam particle backgrounds, as estimated in section 6, ageing considerations would make a reduction in chamber voltage advisable during injection.

All the beam-related backgrounds considered above are potential problems for the electrostatic separators. The separator plates should be well shielded from synchrotron radiation and scattered beam particles to prevent sparking, which could cause beam loss, during both normal running and injection.

REFERENCES

1. J. Gonichon *et al., LAL/RT 90-02.*
2. R. Schindler, *proceedings of this meeting.*
3. C. Hearty, *SLAC B-Factory Note 73.*
4. Blinov *et al., Nucl. Instr. Methods* A273, 31, (1988).